

# Chronic Degeneration Leads to Poor Healing of Repaired Massive Rotator Cuff Tears in Rats

Megan L. Killian,<sup>\*</sup> PhD, Leonardo M. Cavinatto,<sup>\*†</sup> MD, Samuel R. Ward,<sup>‡§||</sup> PT, PhD, Necat Havlioglu,<sup>¶</sup> MD, PhD, Stavros Thomopoulos,<sup>\*\*</sup> PhD, and Leesa M. Galatz,<sup>\*\*</sup> MD  
*Investigation performed at the Department of Orthopaedic Surgery, Washington University, St Louis, Missouri, USA*

**Background:** Chronic rotator cuff tears present a clinical challenge, often with poor outcomes after surgical repair. Degenerative changes to the muscle, tendon, and bone are thought to hinder healing after surgical repair; additionally, the ability to overcome degenerative changes after surgical repair remains unclear.

**Purpose/Hypothesis:** The purpose of this study was to evaluate healing outcomes of muscle, tendon, and bone after tendon repair in a model of chronic rotator cuff disease and to compare these outcomes to those of acute rotator cuff injuries and repair. The hypothesis was that degenerative rotator cuff changes associated with chronic multitendon tears and muscle unloading would lead to poor structural and mechanical outcomes after repair compared with acute injuries and repair.

**Study Design:** Controlled laboratory study.

**Methods:** Chronic rotator cuff injuries, induced via detachment of the supraspinatus (SS) and infraspinatus (IS) tendons and injection of botulinum toxin A into the SS and IS muscle bellies, were created in the shoulders of rats. After 8 weeks of injury, tendons were surgically reattached to the humeral head, and an acute, dual-tendon injury and repair was performed on the contralateral side. After 8 weeks of healing, muscles were examined histologically, and tendon-to-bone samples were examined microscopically, histologically, and biomechanically and via micro-computed tomography.

**Results:** All repairs were intact at the time of dissection, with no evidence of gapping or ruptures. Tendon-to-bone healing after repair in our chronic injury model led to reduced bone quality and morphological disorganization at the repair site compared with acute injuries and repair. SS and IS muscles were atrophic at 8 weeks after repair of chronic injuries, indicating incomplete recovery after repair, whereas SS and IS muscles exhibited less atrophy and degeneration in the acute injury group at 8 weeks after repair. After chronic injuries and repair, humeral heads had decreased total mineral density and an altered trabecular structure, and the repair had decreased strength, stiffness, and toughness, compared with the acute injury and repair group.

**Conclusion:** Chronic degenerative changes in rotator cuff muscles, tendons, and bone led to inferior healing characteristics after repair compared with acute injuries and repair. The changes were not reversible after repair in the time course studied, consistent with clinical impressions.

**Clinical Relevance:** High retear rates after rotator cuff repair are associated with tear size and chronicity. Understanding the mechanisms behind this association may allow for targeted tissue therapy for tissue degeneration that occurs in the setting of chronic tears.

**Keywords:** shoulder; rotator cuff; fatty degeneration; rotator cuff repair

The surgical repair of torn rotator cuff tendons is a clinical challenge, as poor healing often results in failure of healing and poor clinical outcomes.<sup>10,22</sup> The capacity for the rotator cuff to heal after repair is dependent on a variety of factors, including tear chronicity, patient age, and severity of injury.<sup>10,20,63</sup> Chronic tears are characterized by degenerative changes, including an accumulation of intramuscular and myocellular fat deposits, fibrosis, and atrophy of

muscles,<sup>9,21,26,33,43-45,48</sup> loss of tendon organization, and decrease in bone density.<sup>28</sup> The effect of tissue degeneration on subsequent repair characteristics is undefined. In addition, while chronic degeneration is presumed irreversible, the effect of a repair on rotator cuff muscle and tendon degeneration has not been studied in depth. While it is generally accepted that rotator cuff repair heals better in an acute setting before chronic degeneration alters the morphological structure of the tendon and muscle, the healing characteristics of chronic tears are poorly understood.

The majority of clinically translatable animal studies of rotator cuff tears and repair have used an acute, single-tendon injury with immediate repair, which is

representative of the fairly successful clinical case of rotator cuff injuries in healthy patients younger than 60 years.<sup>42</sup> Nonetheless, such preclinical studies have described several different types of animal models, including those in rodents,<sup>3,31,35,36,41,63</sup> sheep,<sup>16</sup> goats,<sup>38</sup> and canines,<sup>7,8</sup> to explore healing outcomes after repair. These models often show that the rotator cuff healing process after repair leads to the formation of scar tissue rather than the regeneration of normal tendon inserting into bone across mineralized fibrocartilage.<sup>16,51,61</sup> Functionally, material and structural properties, such as stiffness, collagen organization, and strength, of healing tissue are vastly inferior compared with preinjury levels.<sup>13,61</sup> Additionally, several studies have evaluated degenerative changes after chronic tendon detachment,<sup>5,34,36,52-54</sup> as well as repair of chronic tears,<sup>5,12,25,31,32</sup> utilizing iterations of these established animal models. For example, supraspinatus (SS) tenotomy leads to increased fibrogenic extracellular matrix gene expression in tendon cells as well as tendon disorganization.<sup>32</sup> Likewise, chronic detachment of both the SS and infraspinatus (IS) tendons can lead to substantial muscle and bone changes in a rodent model of rotator cuff disease, and these changes are magnified in the presence of short-term muscle paralysis.<sup>56,57</sup> A delay in repair after a single-tendon (ie, SS) injury of 3 weeks has been associated with a marked decrease in bone density, decreased material properties, and impaired organization.<sup>12</sup> A delay in rotator cuff repair after a single-tendon (ie, SS) injury led to increased repair site tension, which was strongly correlated with repair site stiffness, strength, and increased cross-sectional area.<sup>18</sup> While the rodent has been used as a model system for chronic tears, the severity of degeneration in muscle, tendon, and bone in the single-tendon injury model does not compare well with the degeneration observed in older patients with chronic tears. Therefore, atrophy and fibrosis have been accelerated in such models using botulinum toxin A<sup>34,57</sup> or suprascapular nerve injuries<sup>36</sup> to induce short-term paralysis or permanent muscle paralysis, respectively.

In the present study, botulinum toxin A was delivered at the time of SS and IS release to induce chronic degenerative changes to the muscle, tendon, and bone. Rotator cuff repair was performed 8 weeks after injury, with contralateral acute release and repair performed at the same time for comparison. The purpose of this study was to investigate the effects of chronic tissue degeneration on repair biomechanics, bone morphometry, and muscle atrophy by comparing acute versus chronic repairs in a rodent model of rotator cuff repair. We hypothesized that degenerative rotator cuff changes associated with chronic multitendon

tears and muscle unloading would lead to poor structural and mechanical outcomes after repair compared with acute injuries and repair of rotator cuff insertion sites.

## METHODS

### Animal Model

Adult, male Sprague Dawley rats (N = 17) were used, as approved through Washington University's animal studies committee. At time zero, all animals underwent unilateral, dual tenotomy of the SS and IS tendons in their right shoulders<sup>31,34,56,57</sup> under anesthesia (isoflurane carried by 2% oxygen). The SS and IS were surgically exposed, injected with 2.5 U of botulinum toxin A each (50  $\mu$ L total volume, diluted in saline), and sharply detached from the bone at their fibrocartilaginous insertions. A botulinum toxin A injection was used to accelerate atrophy and fibrosis commonly seen in chronic tears<sup>31,34,56,57</sup> but did not induce a permanent injury. The contralateral limb underwent a sham operation, including exposure of both tendons and closure of the skin incision using 4-0 Vicryl (Ethicon Inc). Eight weeks after the experimentally induced injury and injection, the right side was repaired (chronic injury and repair group). The left side underwent acute SS and IS injuries, followed by acute repair (acute injury and repair group). This design allowed a side-to-side comparison of tendon-to-bone healing after repair of a chronic tear compared with a contralateral acute injury and repair. The 8-week time point was chosen to evaluate tendon properties after the period of potential early failure of healing. For the repair procedure, individual tendon stumps were grasped using 5-0 Prolene sutures (Ethicon Inc) and a modified Mason-Allen stitch. The insertion site was gently debrided with a bur to remove soft tissue remnants. Individual sutures for the SS and IS tendons were then passed through a bone tunnel that was drilled in an anteroposterior orientation close to the greater tuberosity of the proximal humerus. Sutures were then tied to reapproximate individual tendon ends to their respective anatomic insertions on the humeral head. After repair surgeries, bupivacaine hydrochloride (0.05 mg/kg) was administered to the injury site, and animals were allowed free cage activity until they were sacrificed via carbon dioxide asphyxiation at 8 weeks after repair.

### Micro-Computed Tomography

Rotator cuff tendons were dissected from the surrounding musculature, and care was taken to maintain SS and IS tendon attachments to the proximal humerus. Repair

#Address correspondence to Stavros Thomopoulos, PhD, and Leesa M. Galatz, MD, Department of Orthopaedic Surgery, Washington University, 660 South Euclid, Campus Box 8233, St Louis, MO 63110, USA (emails: ThomopoulosS@wudosis.wustl.edu; galatzl@wudosis.wustl.edu).

\*Department of Orthopaedic Surgery, Washington University, St Louis, Missouri, USA.

<sup>†</sup>Orthopaedics and Traumatology, University of São Paulo, São Paulo, Brazil.

<sup>‡</sup>Department of Radiology, University of California, San Diego, La Jolla, California, USA.

<sup>§</sup>Department of Orthopaedic Surgery, University of California, San Diego, La Jolla, California, USA.

<sup>||</sup>Department of Bioengineering, University of California, San Diego, La Jolla, California, USA.

<sup>¶</sup>John Cochran Division, St Louis Veterans Affairs Medical Center, St Louis, Missouri, USA.

One or more of the authors has declared the following potential conflict of interest or source of funding: The study was supported by the National Institutes of Health (grants R01 AR057836, P30 AR057235, and R24 HD050837).

integrity was determined at gross dissection as the qualitative amount of retraction of the SS and IS tendons from their native insertion sites. Tendon-bone units were immediately fixed in 4% paraformaldehyde for 48 hours and subsequently scanned in air using micro-computed tomography (micro-CT) (Scanco  $\mu$ CT40; cone beam, 20- $\mu$ m voxel size, 45 kV, 177  $\mu$ A, 300-millisecond integration time). After scanning, the tendon cross-sectional area was measured for both the SS and IS. The tendon-to-bone attachment was qualitatively assessed for mineral defects and bone quality in 2-dimensional reconstructions. Additionally, the following bone morphometric outcomes were determined for the trabecular bone of the humeral head, proximal to the growth plate, excluding the cortical bone: bone volume (BV) percentage (BV/total volume), tissue mineral density (TMD), trabecular bone parameters (trabecular number, trabecular spacing, trabecular thickness), and connectivity density.

### Tendon-to-Bone Mechanics

After sacrifice, intact carcasses of rats used for biomechanical tests were immediately frozen at  $-20^{\circ}\text{C}$  until tests were performed ( $n = 12$ ). Carcasses were thawed, and SS/IS tendon-to-bone attachments, including the entire humerus, were dissected as single units. Repair integrity was assessed, and sutures were cut to remove their load-carrying capacity during uniaxial tensile tests (and hence evaluate only the biomechanics of the healing tissue). Cross-sectional areas at the insertion for both the SS and IS were measured using micro-CT. To ensure stability of the humeral head and prevent growth plate failures during tests, a hole was drilled through the diaphysis of the humerus, and a steel wire was passed through the hole and wrapped around the humeral head medial and posterior to the SS and IS attachments, respectively. Humeri were then potted in stainless steel square tubing using poly(methyl methacrylate), and surface markings were applied via sputter coating to the epitenon and scar using fresh hematoxylin. Samples were held in custom fixtures at the base of a saline bath at  $37^{\circ}\text{C}$ . To determine the mechanical properties of the IS and SS attachments, a non-damaging tensile test was first performed on the IS, followed by a tensile test to failure of the SS (Instron 5866). Tendons were gripped using thin film grips (Imada Inc) as follows: Alignment of the IS was ensured for uniaxial loading, and IS tendons were loaded to a 0.2-N tare load. Gauge length ( $L_0$ ) was measured and used to calculate the grip-to-grip strain ( $L/L_0$ ). IS tendons were then preconditioned for 5 cycles of a 5% strain ramp at 0.2%/s, followed by a rest interval (300 seconds), subjected to stress relaxation of 5% strain at a 50%/s ramp speed for 300 seconds, a subsequent rest interval (300 seconds), and finally uniaxially loaded to 3 N at 0.2%/s. After loading of the IS, samples were realigned in the bottom fixture for uniaxial testing of the SS tendon. A similar preconditioning protocol was applied to SS tendons, followed by stress relaxation, a rest interval, and uniaxial load to failure at 0.2%/s. Measured and calculated biomechanical outcomes were stiffness (N/mm), maximum load to failure ( $\text{load}_{\text{max}}$ , N), modulus of elasticity (E, MPa), maximum stress to failure

( $\text{stress}_{\text{max}}$ , MPa), toughness (measured as the area under the stress-strain curve through  $\text{stress}_{\text{max}}$ , MPa), and ultimate strain (strain at maximum load, %). Failure testing resulted in alteration of both insertion sites; therefore, only the SS was tested to failure.

### Muscle Histology

The SS and IS muscle biopsy specimens were obtained from the medial aspect of the scapula, exclusive of myotendinous junctions, and pinned to cork at approximate anatomic lengths. Biopsy specimens were then flash frozen in liquid nitrogen-cooled isopentane and sectioned at 5- $\mu$ m thickness. Sections were stained with wheat germ agglutinin to label the sarcolemma, and the muscle fiber cross-sectional area was measured using ImageJ open-source software ( $n = 5$  per muscle per group) (National Institutes of Health).<sup>24</sup>

### Tendon-to-Bone Histology

After micro-CT, tendon-to-bone specimens designated for histological analyses ( $n = 5$ ) were decalcified in formic acid (Immunocal; Immunotec Inc), paraffin embedded, and sectioned at a 10- $\mu$ m thickness. Sections were subsequently stained using safranin O for proteoglycan coverage as well as hematoxylin and eosin for pathological analysis. Stained sections were analyzed in a blinded fashion by an experienced pathologist (N.H.) using previously established criteria, detailed as follows.<sup>11-14,31,40</sup> Inflammation (cellularity, mononuclear/polynuclear cell density), vascularity, tendon-bone continuity, and bone resorption were assessed. Cellularity was assigned a score of + through +++++, and mononuclear cells and polymorphonuclear cells were assigned a score of + through +++, with + = <50 cells/high-powered field of view (HPF); ++ = 50-100 cells/HPF; +++ = 100-150 cells/HPF; and +++++ = >150 cells/HPF. Vascularity was assigned a score of + through +++, with + = <10 vessels/HPF; ++ = 11-20 vessels/HPF; and +++ = >20 vessels/HPF. Foreign bodies were scored as present (+) or not present (-). Tendon continuity and entheses continuity were scored as follows: + = tendon/entheses thickness near the attachment site was <25%; ++ = tendon/entheses thickness near the attachment site was 25%-50%; or +++ = tendon/entheses thickness near the attachment site was >50%. Collagen organization was assigned a score of - through +++, with - = tightly packed parallel bundle of collagen with slight waviness; + = slight separation of fibers with increased patchy waviness; ++ = some loss of orientation of collagen bundles and loss of orientation of nuclei in relation to collagen; and +++ = complete loss of organization. Fibrocartilage and bone island detection at the attachment was assessed as either present (+) or not present (-).

### Statistical Analyses

The sample size was calculated using a priori power analysis from expected differences between the chronic and acute groups, informed by previous studies in our

TABLE 1  
Histomorphology for SS Tendon-to-Bone Attachments After Acute and Chronic Injuries and Repairs<sup>a</sup>

Group	Cellularity	Vascularity	FB	PMN	Mono	Tendon Continuity	Enthesis Continuity	Collagen Organization	Fibrocartilage/Bone Island
Acute injury and repair	+++	+	+	+	++	++	++	++	+
Chronic injury and repair	++	++	+	+	+	+++	+++	++	+

<sup>a</sup>Scoring (+, ++, +++) is described in detail in the Methods section. FB, foreign bodies; Mono, mononuclear cells; PMN, polymorphonuclear cells; SS, supraspinatus.

TABLE 2  
Bone Morphometry of Proximal Humeral Trabeculae for Acute and Chronic Injuries and Repairs<sup>a</sup>

Group	Total Volume, mm <sup>3</sup>	Trabecular Bone Volume, mm <sup>3</sup>	Bone Volume/Total Volume, %	Connectivity Density
Acute injury and repair	31.4 (24.3-38.5)	11.8 (7.6-16.0)	37 (29-44)	45.7 (37.2-54.1)
Chronic injury and repair	29.7 (22.0-37.5)	8.7 (4.3-13.1)	28 (19-36) <sup>b</sup>	42.3 (32.7-51.9)

<sup>a</sup>Results are reported as mean (95% CI).

<sup>b</sup>Statistically significant difference between the chronic and acute groups ( $P = .019$ ).

laboratory investigating rotator cuff healing.<sup>12,31,40</sup> Paired *t* tests were used to compare quantitative outcomes for bone morphometry, biomechanical properties, and muscle fiber cross-sectional area and heterogeneity ( $P < .05$  significance). Data are presented graphically as mean with positive error bars representing the upper 95% CI, or in tables as mean (95% CI). Histological outcomes presented in Table 1 were semiquantitative in nature; therefore, these data were presented in a nonnumerical format (+, ++, +++) and described qualitatively.

## RESULTS

All SS and IS tendons were intact and congruent at the time of dissection, regardless of injury duration before repair. Gross investigation of repaired tendons indicated no gap formation or suture disruption for either the acute or chronic repair group. Morphologically, the acute injury and repair group had robust muscle bellies and normal, round humeral heads. However, gross anatomic differences were present in the chronic injury and repair group, as these shoulders had smaller rotator cuff muscles and flattened anterior/posterior humeral head shapes. Rodents maintained open growth plates throughout the duration of this study, and therefore, bony changes may have developed from remodeling secondary to altered muscle forces across the joint.

From micro-CT reconstructions, proximal humeri from the acute injury and repair group maintained congruent cortical bone and medial compartment trabeculae (Figure 1A). However, bone quality in the proximal humeri from the chronic injury and repair group was diminutive, with loss of cortical bone closest to the reattachment location (Figure 1B). Additionally, healed attachments of the chronic injury and repair group demonstrated a qualitative increase in heterotopic ossification (Figure 1B, arrowheads) compared with the acute injury and repair group (Figure 1A,

arrowhead). Quantitatively, proximal humeri from the chronic injury and repair group had approximately 25% less trabecular bone volume compared with the acute injury and repair group (Table 2), and TMD was significantly reduced in the chronic injury and repair group compared with the acute injury and repair group (Figure 1C). There were no significant differences in the volume of trabecular bone of the humeral head for either group; however, the chronic injury and repair group had 9% less bone volume percentage (BV/total volume) compared with the acute injury and repair group (Table 2). There were significantly fewer trabeculae (Figure 1D) and increased trabecular spacing (Figure 1E) in the chronic injury and repair group compared with the acute injury and repair group, but no differences were observed quantitatively in the thickness of present trabeculae (Figure 1F). No differences in connectivity density were observed between groups (Table 2).

Chronic injuries and repair led to impaired mechanical outcomes of the SS tendon-to-bone attachment compared with acute injuries and repair (Figure 2). No differences between injury duration were observed in IS tendon-to-bone mechanical properties (eg, stiffness [Figure 2A] and modulus of elasticity [Figure 2C]) when loaded to 2 N. However, SS attachments of the chronic injury and repair group were significantly less stiff (Figure 2A) and had a lower modulus of elasticity (Figure 2C) compared with SS attachments of the acute injury and repair group. Additionally, tendon-to-bone attachments of the chronic injury and repair group failed at lower loads (Figure 2B) compared with the acute injury and repair group, and the chronic injury and repair group demonstrated significantly lower ultimate strength (Figure 2D) and toughness (Figure 2E) compared with the acute injury and repair group. There were no significant differences in ultimate strain between groups (Figure 2F).

Gross observations of decreases in muscle mass were consistent with decreased muscle fiber cross-sectional areas in the chronic injury and repair group (Figure 3A',

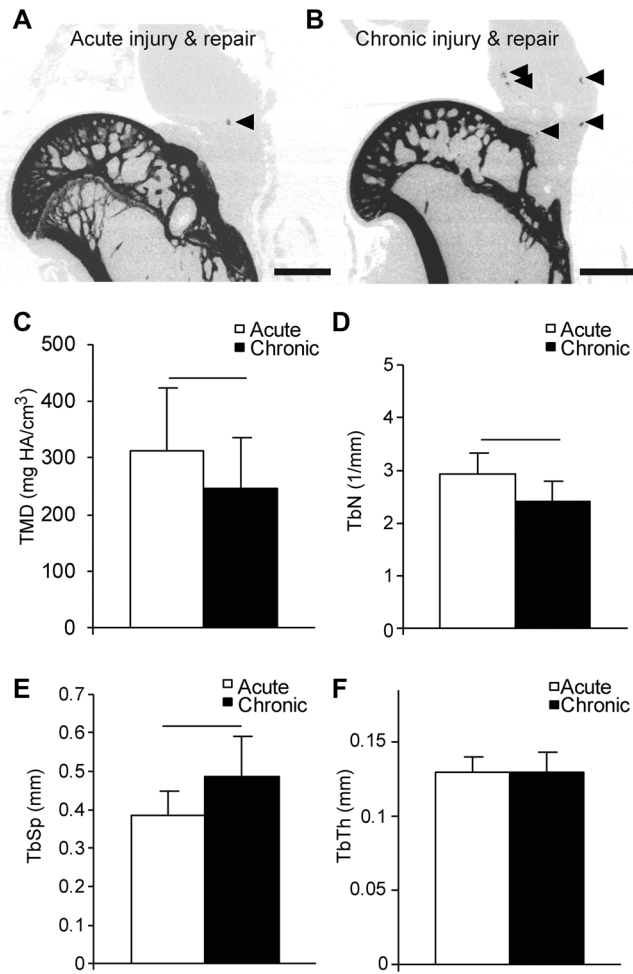


**Figure 1.** Representative micro-computed tomographic reconstructions of 0.5 mm-thick coronal sections of proximal humeri after (A) acute injuries and repair and (B) chronic injuries and repair. Arrowheads indicate localized heterotopic ossifications in the tendon/scar. Trabecular bone morphometric outcomes for (C) tissue mineral density (TMD), (D) trabecular number (TbN), and (E) trabecular spacing (TbSp) were significantly different between acute and chronic groups. (F) No differences in trabecular thickness (TbTh) between groups were observed. Lines indicate significant differences between acute and chronic groups ( $P < .05$ ). Scale bar in A and B = 2 mm. Data are presented as mean + upper 95% CI.

SS muscle) compared with the acute injury and repair group (Figure 3A, SS muscle). Both SS and IS muscles from the acute injury and repair group had significantly larger muscle fiber cross-sectional areas compared with the respective muscles in the chronic injury and repair group (Figure 3B). No differences in fiber size heterogeneity were measured between the acute or chronic injury and repair groups (Figure 3C).

Semiquantitative assessments of histological outcomes for the acute injury and repair group and chronic injury and repair group are detailed in Table 1. Morphologically,

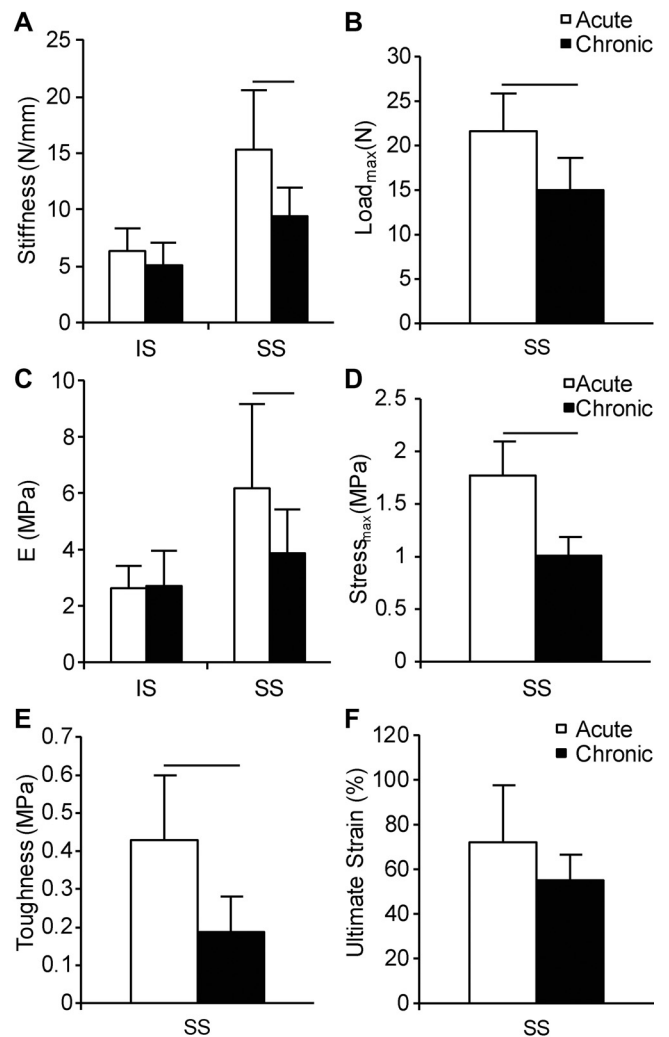


**Figure 2.** Mechanical outcomes for uniaxial tensile tests of infraspinatus (IS) and supraspinatus (SS) tendon-to-bone attachments of the acute injury and repair group and chronic injury and repair group. (A) Stiffness (N/mm) for IS and SS attachments, (B) maximum load to failure (Load<sub>max</sub>, N) for SS attachments, (C) Young modulus (MPa) for IS and SS attachments, (D) maximum stress to failure of SS attachments (Stress<sub>max</sub>, MPa), (E) toughness (MPa) of SS attachments, and (F) ultimate strain (%) of SS attachments. Lines indicate significant differences between acute and chronic groups ( $P < .05$ ). Data are presented as mean + upper 95% CI.

tendon-to-bone attachments in both the acute and chronic injury and repair groups demonstrated transitional fibrocartilage with congruent, continuous collagen fibers from the tendon into the bone (Figure 4). After chronic injuries and repair, the tendon-to-bone attachments demonstrated increased vascularity and less cellularity compared with attachments of the acute injury and repair group (Figure 4, B and B', and Table 1). The SS tendon and enthesis were both thicker near and at the attachment site after chronic injuries and repair compared with acute injuries

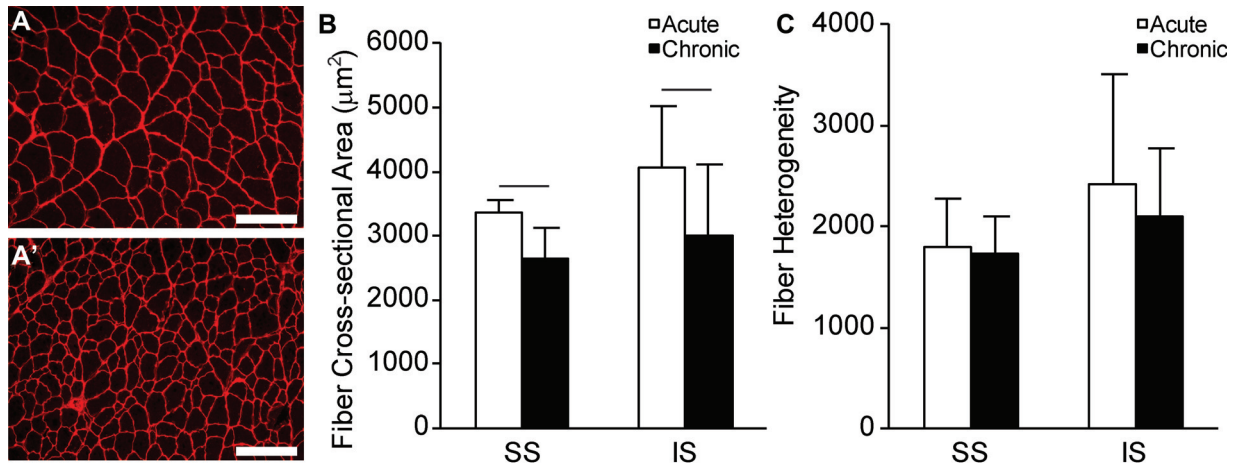


**Figure 3.** Representative fiber cross-sectional area of the supraspinatus (SS) muscle after (A) acute injuries and repair and (A') chronic injuries and repair. (B) SS and infraspinatus (IS) fiber cross-sectional areas ( $\mu\text{m}^2$ ) and (C) fiber heterogeneity for the acute injury and repair group and chronic injury and repair group. Scale bar in A and A' = 200  $\mu\text{m}$ . Lines in B indicate significant differences between acute and chronic groups ( $P < .05$ ). Data are presented as mean + upper 95% CI.

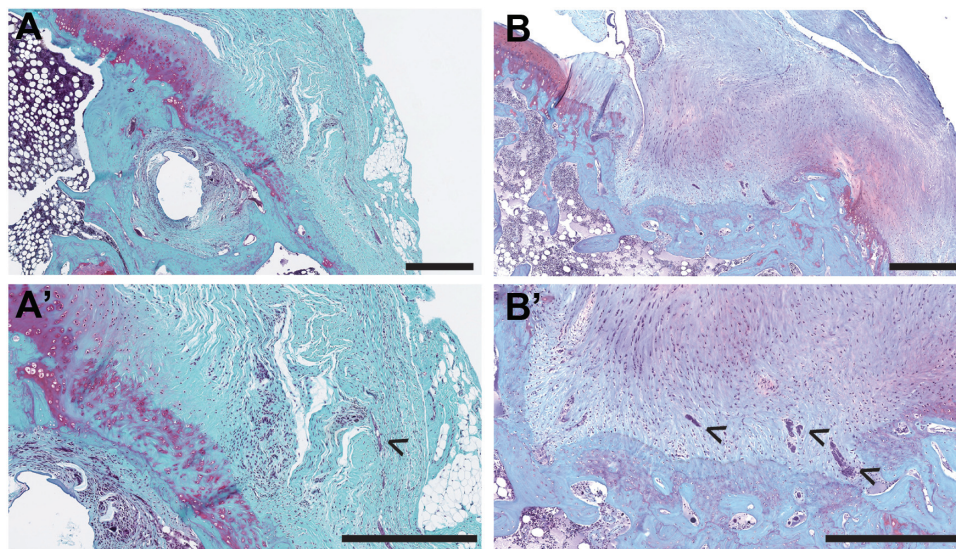


**Figure 4.** Histomorphological comparisons of tendon-to-bone attachments after (A, A') acute injuries and repair and (B, B') chronic injuries and repair. Safranin O–stained sections showed increased vascularity (B', arrowheads) after chronic injuries and repair compared with (A') acute injuries and repair. Scale bar = 500  $\mu\text{m}$ . A' and B' represent higher magnification images of A and B, respectively.

and repair (Table 1). The acute injury and repair group demonstrated comparable or slightly higher amounts of mononuclear cells and polymorphonuclear cells (Table 1). No differences were observed in the presence of fibrocartilage bone islands near the attachment between acute and chronic groups (Table 1).

**DISCUSSION**

This study demonstrated that massive, chronic rotator cuff tears in a rodent model have some healing capacity;

however, healing is inferior to acutely repaired tears. The study design allowed within-animal, paired comparisons between acutely and chronically repaired rotator cuffs, and no gapping or repair site ruptures complicated the comparison (unlike a previous study on the repair of chronically degenerated rotator cuffs<sup>31</sup>). After chronic injuries and repair, the healing rotator cuff was in continuity with the bony insertion but was more disorganized, was fibrotic, and had qualitatively more heterotopic ossification in the tendon/muscle compared with the acute injury and repair group. The increased presence of heterotopic ossification in the chronic group could potentially be caused by

a multitude of factors, including increased duration of tendon injury, altered mechanical loading of the tendons and muscles, and acute neural dysfunction. Bone quality and quantity of the proximal humeri were reduced in the chronic injury and repair group compared with the acute injury and repair group, and the structural changes translated into reduced functional (ie, mechanical) outcomes. It is widely accepted that chronic tears are more difficult to repair because of long-standing retraction and structural changes to the muscle tissue, and healing is not guaranteed after repair.<sup>2,10</sup> The current animal study supports this clinical impression, demonstrating the structural and functional implications associated with healing after acute or chronic, degenerative tears. In this study, the chronic tears were also more difficult to repair in this model compared with the acute tendon injuries mostly because of increased scar formation, tendon retraction, and loss of bone. Results established specific differences between acute and chronic injuries that can begin to explain the clinical problems associated with the repair of chronically degenerated rotator cuffs. While degenerative changes to the tendon and muscle caused by unloading clearly affected the mechanical properties of the repair, the current study was not designed to determine the mechanism by which this occurred. A number of possibilities by which this occurred, all the subject of future study, include bone loss leading to poor tendon-bone anchoring, tendon degeneration leading to poor suture-tendon grasping, and muscle degeneration leading to negative paracrine-mediated soluble signals.

Clinically, poor healing in the chronic setting may arise from multiple sources. Retracted, fibrotic muscles become stiffer, leading to poor mobilization and high tension on the repair site. Previous animal studies in larger animals have demonstrated this in a unilateral chronic model.<sup>5,15</sup> Changes in rotator cuff muscle physiology, induced by tendon release and muscle retraction in the scapular fossa, can also lead to increased passive stiffness and increased repair site tension.<sup>17,18,57</sup> Additionally, retraction can potentially lead to suprascapular nerve impingement and palsy.<sup>1,6,39,62</sup> In previous work, it has been found that a single injection of botulinum toxin A after SS and IS tenotomy could lead to acute muscle changes such as increased muscle fiber bundle stiffness and collagen content at 8 weeks after injury, with such functional and biochemical changes associated with muscle paralysis being recovered by 16 weeks after injury.<sup>57</sup> Likewise, Hettrich et al<sup>23</sup> showed that there were no differences in the SS muscle volume at 24 weeks after an injection of botulinum toxin A with an SS tendon injury and immediate repair compared with an uninjected injury and repair. Additionally, Ma et al<sup>37</sup> demonstrated that botulinum-induced denervation of the gastrocnemius in juvenile rats was maintained for 2 weeks and that muscle volume was 70% to 90% recovered by 2 months after the injection. Therefore, it was expected that the effect of botulinum toxin A on skeletal muscle would subside by the time of sacrifice in this study. However, the quality of SS and IS muscles, as measured by fiber cross-sectional area and mass, were not comparable between the acute and chronic sides, suggesting that the muscle in the chronic group did not fully recover or

continued to atrophy during the additional 8 weeks after the repair period. This implies that incomplete muscle recovery is related to chronic tendon detachment and repair, consistent with the incomplete reversal of muscle atrophy seen clinically. Finally, damage to the muscle during tendon retraction after a tear may also impair healing.

In the present study, chronic injuries also affected tendon and bone quality, and these changes persist despite repair. Loss of collagen organization of the rotator cuff tendons after chronic detachment can lead to decreased mechanical properties.<sup>19</sup> Elevated bone loss at the humeral head was observed after chronic injuries and repair, and osteopenia has previously been correlated with the severity and chronicity of rotator cuff retraction in both the clinical setting and in animal models.<sup>3,12,31,56</sup> These structural and compositional changes have combined deleterious effects on the repair strength and function of the healing rotator cuff.

This study has several strengths and limitations. Bilateral comparisons of healing outcomes for both acute and chronic injuries allowed for internal control of the age and physiology of individual rodents, thereby increasing the statistical power of the comparisons made in this study. However, the present study design was limited, as it did not compare normal, uninjured rotator cuff health to that of the acute or chronic injury and repair cases. In addition, bilateral surgeries may have influenced the forelimb weightbearing activity, both before repair and after repair. Specifically, animals may have used their sham-operated limb more than their chronically injured limb in the period before surgical repair. This may have led to adaptations in bone, tendon, and muscle strength in the sham side before the acute injury and repair. Conversely, the animals may have continued to utilize their acutely injured shoulder more than their chronically injured shoulder after repair. Nonetheless, all repairs in the chronic and acute groups were intact at the time of sacrifice. Therefore, we concluded that even with possible asymmetric loading between shoulders, the outcomes after repair were substantially impaired after chronic injuries compared with acute injuries. Comparisons between healthy and chronically degenerative rotator cuffs have been previously made.<sup>56,57</sup> It has been previously shown that rodent rotator cuff muscle mass continues to increase with increasing rodent age,<sup>60</sup> and such growth is blunted when muscle and tendon injuries are present.<sup>56</sup> In the present study, we expected that the size, shape, and health of the rotator cuff complex were better for the acute injury group compared with the chronic injury group at the time of repair. While the overwhelming changes in the muscle and bone architecture after chronic injuries likely drive such differences, it is possible that the age of the rodent at the time of injury may also be a contributing factor to rotator cuff health. Specifically, at the time of repair, rotator cuff complexes in the acute injury side were 8 weeks more mature than those of the chronic injury side. The muscle, tendon, and bone in the acute injury side may have had a somewhat different response to injuries than the chronic side had at 8 weeks prior. Nonetheless, this potential pitfall may strengthen our findings that chronic injuries heal poorly compared with acute injuries, even when the acute injury is at a later chronological age.

The use of short-term chemical paralysis to drive atrophy and fibrosis in the rotator cuff muscles is both a strength and limitation. While this approach does not re-create the pathogenesis of rotator cuff disease seen clinically, it does reproduce the endpoint of the disease (namely, rotator cuff fibrosis and fatty degeneration); the use of a rodent animal model prevents the pursuit of time courses relevant to chronic changes in the human shoulder.<sup>43,44</sup> Botulinum toxin A caused atrophy,<sup>23,37</sup> fibrosis,<sup>57</sup> loss of force production,<sup>59</sup> and increased stiffness<sup>57</sup> in the muscle, all of which are problems encountered clinically in rotator cuff disease. These changes were substantially greater with the use of botulinum toxin A than with tendon detachment alone.<sup>34,56,57</sup> Although botulinum toxin A was used to induce atrophy in the rotator cuff muscles, it has been established that this toxin does not compromise surrounding tissues and is reversible.<sup>23,37,47</sup> Recent work showed that the transcriptional regulation of repair and atrophy were modulated by botulinum toxin acutely after an injection, but changes returned to baseline by 12 weeks after the injection in the rabbit tibialis anterior.<sup>47</sup> Of note is that botulinum toxin paralysis does not lead to profound fatty accumulation in intact rodent rotator cuff muscles. Rather, denervation, either via neurotoxin or neurotomy, is necessary to induce such fatty, atrophic changes.<sup>34</sup> The administration of botulinum toxin mimics, but does not replicate, the outcomes seen in the chronic condition clinically.

An additional limitation is the use of a rodent model. The size and age of the animals do not approximate those of humans with rotator cuff disease. Chronic repairs were challenging in this small animal model, but observable differences were great enough, given the relatively small sample size, that a larger sample size would unlikely change the results. Additionally, the duration of injury, as well as the duration of healing after repair, may limit the strength of our conclusions. For this study, we chose to use a single time point of 8 weeks after repair to evaluate tendon properties, after a period of potential early failure of healing, while limiting the duration of the study, given the relatively short life span of rodents (~2-3 years). The duration of injury utilized for the present study does not directly translate to the duration that is likely required for chronic, degenerative changes to be observable clinically. However, little is known regarding the natural onset and progression of chronic, degenerative changes in patients with asymptomatic rotator cuff tears.<sup>30,46,63</sup> Findings from previous work by our group and others have shown that profound degenerative changes to the muscle, tendon, and bone after chronic injuries occur within 8 weeks after injury, and these changes are comparable in the pathophysiology with that of chronic rotator cuff tears seen clinically.<sup>27,31,34,36,56,57</sup> The rodent model of rotator cuff injury and repair is a well-established and clinically relevant model for studying tendon-to-bone development, degeneration, and healing.\*\* Additionally, the rodent model is well established for use in the study of rotator

cuff disease, as it is anatomically similar to the human shoulder<sup>58</sup> and is arguably the best anatomically relevant model, aside from macaque, for studying the rotator cuff. Rodents continue to grow skeletally throughout life, and it is expected that, over the duration of this experiment, muscle mass and muscle size would increase approximately 30%.<sup>60</sup> This continuation of growth may influence muscle- and bone-related outcomes that are compared between acute and chronic groups and should therefore be interpreted with caution. Finally, while it is generally accepted that muscle physiology is compromised in the chronic setting, the current study demonstrated clear differences in all tissues of the rotator cuff (including bone and tendon), culminating in a poorer repair independent of age-related or systematic adaptations after injury and degeneration. These data serve as a basis for the further study of treatment modalities to address the individual deficiencies.

## CONCLUSION

Repair of massive chronic rotator cuff tears led to poor healing compared with repair of acute injuries in the rat model. Atrophy and degeneration were achieved using tenotomy and chemical paralysis to model the chronic tear scenario. Poor muscle quality, tendon mechanics, and bone density in chronically degenerated rotator cuffs led to inferior healing at the tendon-to-bone attachment.

## ACKNOWLEDGMENT

Tendon histology was performed by Crystal Idelburg, HT (ASCP).

## REFERENCES

1. Albritton M, Graham R, Richards R, Basamania C. An anatomic study of the effects on the suprascapular nerve due to retraction of the supraspinatus muscle after a rotator cuff tear. *J Shoulder Elbow Surg.* 2003;12(5):497-500.
2. Boileau P, Brassart N, Watkinson D, et al. Arthroscopic repair of full-thickness tears of the supraspinatus: does the tendon really heal? *J Bone Joint Surg Am.* 2005;87(6):1229-1240.
3. Cadet ER, Hsu J, Levine W, et al. The relationship between greater tuberosity osteopenia and the chronicity of rotator cuff tears. *J Shoulder Elbow Surg.* 2008;17(1):73-77.
4. Cadet ER, Vorys GC, Rahman R, et al. Improving bone density at the rotator cuff footprint increases supraspinatus tendon failure stress in a rat model. *J Orthop Res.* 2010;28(3):308-314.
5. Coleman SH, Fealy S, Ehteshami JR, et al. Chronic rotator cuff injury and repair model in sheep. *J Bone Joint Surg Am.* 2003;85(12):2391-2402.
6. Costouros JG, Porramatikul M, Lie DT, Warner JJ. Reversal of suprascapular neuropathy following arthroscopic repair of massive supraspinatus and infraspinatus rotator cuff tears. *Arthroscopy.* 2007;23(11):1152-1161.
7. Derwin K, Baker A, Codsí M, Ianotti J. Assessment of the canine model of rotator cuff injury and repair. *J Shoulder Elbow Surg.* 2007;16(5):S140-S148.
8. Derwin KA, Badylak SF, Steinmann SP, Iannotti JP. Extracellular matrix scaffold devices for rotator cuff repair. *J Shoulder Elbow Surg.* 2010;19(3):467-476.

\*\*References 4, 17, 19, 23, 29, 36, 49, 50, 55.

9. Fuchs B, Weishaupt D, Zanetti M, et al. Fatty degeneration of the muscles of the rotator cuff: assessment by computed tomography versus magnetic resonance imaging. *J Shoulder Elbow Surg.* 1999;8(6):599-605.
10. Galatz LM, Ball CM, Teefey SA, et al. The outcome and repair integrity of completely arthroscopically repaired large and massive rotator cuff tears. *J Bone Joint Surg Am.* 2004;86(2):219-224.
11. Galatz LM, Charlton N, Das R, et al. Complete removal of load is detrimental to rotator cuff healing. *J Shoulder Elbow Surg.* 2009;18(5):669-675.
12. Galatz LM, Rothermich SY, Zaegel M, et al. Delayed repair of tendon to bone injuries leads to decreased biomechanical properties and bone loss. *J Orthop Res.* 2005;23(6):1441-1447.
13. Galatz LM, Sandell LJ, Rothermich SY, et al. Characteristics of the rat supraspinatus tendon during tendon-to-bone healing after acute injury. *J Orthop Res.* 2006;24(3):541-550.
14. Galatz LM, Silva MJ, Rothermich SY, et al. Nicotine delays tendon-to-bone healing in a rat shoulder model. *J Bone Joint Surg Am.* 2006;88(9):2027-2034.
15. Gerber C, Meyer DC, Schneeberger AG, et al. Effect of tendon release and delayed repair on the structure of the muscles of the rotator cuff: an experimental study in sheep. *J Bone Joint Surg Am.* 2004;86(9):1973-1982.
16. Gerber C, Schneeberger AG, Perren SM, Nyffeler RW. Experimental rotator cuff repair: a preliminary study. *J Bone Joint Surg Am.* 1999;81(9):1281-1290.
17. Gimbel JA, Mehta S, Van Kleunen JP, et al. The tension required at repair to reappose the supraspinatus tendon to bone rapidly increases after injury. *Clin Orthop Relat Res.* 2004;426:258-265.
18. Gimbel JA, Van Kleunen JP, Lake SP, et al. The role of repair tension on tendon to bone healing in an animal model of chronic rotator cuff tears. *J Biomech.* 2006;40(3):561-568.
19. Gimbel JA, Van Kleunen JP, Mehta S, et al. Supraspinatus tendon organizational and mechanical properties in a chronic rotator cuff tear animal model. *J Biomech.* 2004;37(5):739-749.
20. Gladstone J, Bishop J, Lo I, Flatow EL. Fatty infiltration and atrophy of the rotator cuff do not improve after rotator cuff repair and correlate with poor functional outcome. *Am J Sports Med.* 2007;35(5):719-728.
21. Goutallier D, Postel JM, Bernageau J, et al. Fatty muscle degeneration in cuff ruptures: pre- and postoperative evaluation by CT scan. *Clin Orthop Relat Res.* 1994;304:78-83.
22. Harryman DT 2nd, Mack LA, Wang KY, et al. Repairs of the rotator cuff: correlation of functional results with integrity of the cuff. *J Bone Joint Surg Am.* 1991;73(7):982-989.
23. Hettrich CM, Rodeo SA, Hannafin JA, et al. The effect of muscle paralysis using botox on the healing of tendon to bone in a rat model. *J Shoulder Elbow Surg.* 2011;20:688-698.
24. Hulst J, Minamoto V, Lim M, et al. Systematic test of neurotoxin dose and volume on muscle function in a rat model. *Muscle Nerve.* 2014;49(5):709-715.
25. Iannotti JP, Codsí MJ, Kwon YW, et al. Porcine small intestine submucosa augmentation of surgical repair of chronic two-tendon rotator cuff tears: a randomized, controlled trial. *J Bone Joint Surg Am.* 2006;88(6):1238-1244.
26. Itoigawa Y, Kishimoto K, Sano H, et al. Molecular mechanism of fatty degeneration in rotator cuff muscle with tendon rupture. *J Orthop Res.* 2011;29:861-866.
27. Kang J, Gupta R. Mechanisms of fatty degeneration in massive rotator cuff tears. *J Shoulder Elbow Surg.* 2012;21(2):175-180.
28. Kannus P, Leppala J, Lehto M, et al. A rotator cuff rupture produces permanent osteoporosis in the affected extremity, but not in those with whom shoulder function has returned to normal. *J Bone Miner Res.* 1995;10(8):1263-1271.
29. Kawamura S, Ying L, Kim HJ, et al. Macrophages accumulate in the early phase of tendon-bone healing. *J Orthop Res.* 2005;23(6):1425-1432.
30. Keener J, Galatz LM, Teefey S, et al. A prospective evaluation of survivorship of asymptomatic degenerative rotator cuff tears. *J Bone Joint Surg Am.* 2015;97(2):89-98.
31. Killian M, Cavinatto L, Shah S, et al. The effects of chronic unloading and gap formation on tendon-to-bone healing in a rat model of massive rotator cuff tears. *J Orthop Res.* 2014;32(3):439-447.
32. Killian ML, Lim C, Thomopoulos S, et al. The effects of unloading on gene expression of healthy and injured rotator cuffs. *J Orthop Res.* 2013;31(8):1240-1248.
33. Kim H, Dahiva N, Teefey SA, et al. Relationship of tear size and location of fatty degeneration of the rotator cuff. *J Bone Joint Surg Am.* 2010;92(4):829-839.
34. Kim H, Galatz L, Lim C, et al. The effect of tear size and nerve injury on rotator cuff muscle fatty degeneration in a rodent animal model. *J Shoulder Elbow Surg.* 2012;21(7):847-858.
35. Kim HM, Galatz LM, Das R, et al. Musculoskeletal deformities secondary to neurotomy of the superior trunk of the brachial plexus in neonatal mice. *J Orthop Res.* 2010;28(10):1391-1398.
36. Liu X, Manzano G, Kim H, Feeley B. A rat model of massive rotator cuff tears. *J Orthop Res.* 2011;29(4):588-595.
37. Ma J, Elsaidi GA, Smith TL, et al. Time course of recovery of juvenile skeletal muscle after botulinum toxin a injection: an animal model study. *Am J Phys Med Rehabil.* 2004;83(10):774-780.
38. Macgillivray JD, Fealy S, Terry MA, et al. Biomechanical evaluation of a rotator cuff defect model augmented with a bioresorbable scaffold in goats. *J Shoulder Elbow Surg.* 2006;15(5):639-644.
39. Mallon WJ, Wilson RJ, Basamania CJ. The association of suprascapular neuropathy with massive rotator cuff tears: a preliminary report. *J Shoulder Elbow Surg.* 2006;15(4):395-398.
40. Manning CN, Kim HM, Sakiyama-Elbert S, et al. Sustained delivery of transforming growth factor beta three enhances tendon-to-bone healing in a rat model. *J Orthop Res.* 2011;29(7):1099-1105.
41. Massimini D, Singh A, Wells J, et al. Suprascapular nerve anatomy during shoulder motion: a cadaveric proof of concept study with implications for neurogenic shoulder pain. *J Shoulder Elbow Surg.* 2013;22(4):463-470.
42. Matsen F. Rotator-cuff failure. *New Engl J Med.* 2008;358:2138-2147.
43. Melis B, Defranco M, Chuinard C, Walch G. Natural history of fatty infiltration and atrophy of the supraspinatus muscle in rotator cuff tears. *Clin Orthop Relat Res.* 2010;468(6):1498-1505.
44. Melis B, Wall B, Walch G. Natural history of infraspinatus fatty infiltration in rotator cuff tears. *J Shoulder Elbow Surg.* 2010;19(5):757-763.
45. Meyer DC, Pirkel C, Pfirrmann CW, et al. Asymmetric atrophy of the supraspinatus muscle following tendon tear. *J Orthop Res.* 2005;23(2):254-258.
46. Moosmayer S, Tariq R, Stiris M, Smith H-J. The natural history of asymptomatic rotator cuff tears. *J Bone Joint Surg Am.* 2013;95(14):1249-1255.
47. Mukund K, Mathewson M, Minamoto V, et al. Systems analysis of transcriptional data provides insights into muscle's biological response to botulinum toxin. *Muscle Nerve.* 2014;50(5):744-758.
48. Nakagaki K, Ozaki J, Tomita Y, Tamai S. Fatty degeneration in the supraspinatus muscle after rotator cuff tear. *J Shoulder Elbow Surg.* 1996;5(3):194-200.
49. Peltz CD, Dourte LM, Kuntz AF, et al. The effect of postoperative passive motion on rotator cuff healing in a rat model. *J Bone Joint Surg Am.* 2009;91(10):2421-2429.
50. Peltz CD, Sarver JJ, Dourte LM, et al. Exercise following a short immobilization period is detrimental to tendon properties and joint mechanics in a rat rotator cuff injury model. *J Orthop Res.* 2010;28(7):841-845.
51. Rodeo S. Biologic augmentation of rotator cuff tendon repair. *J Shoulder Elbow Surg.* 2007;16(5):S191-S197.
52. Rowshan K, Hadley S, Pham K, et al. Development of fatty atrophy after neurologic and rotator cuff injuries in an animal model of rotator cuff pathology. *J Bone Joint Surg Am.* 2010;92(13):2270-2278.

53. Rubino LJ, Stills HF Jr, Sprott DC, Crosby LA. Fatty infiltration of the torn rotator cuff worsens over time in a rabbit model. *Arthroscopy*. 2007;23(7):717-722.
54. Safran O, Derwin KA, Powell K, Iannotti JP. Changes in rotator cuff muscle volume, fat content, and passive mechanics after chronic detachment in a canine model. *J Bone Joint Surg Am*. 2005;87(12):2662-2670.
55. Sarver JJ, Peltz CD, Dourte L, et al. After rotator cuff repair, stiffness—but not the loss in range of motion—increased transiently for immobilized shoulders in a rat model. *J Shoulder Elbow Surg*. 2008;17(1 Suppl):108S-113S.
56. Sato E, Killian M, Choi A, et al. Architectural and biochemical adaptations in skeletal muscle and bone following rotator cuff injury in a rat model. *J Bone Joint Surg Am*. 2015;97(7):565-573.
57. Sato E, Killian ML, Choi A, et al. Skeletal muscle fibrosis and stiffness increase after rotator cuff tendon injury and neuromuscular compromise in a rat model. *J Orthop Res*. 2014;32(9):1111-1116.
58. Soslowsky LJ, Carpenter JE, DeBano CM, et al. Development and use of an animal model for investigations on rotator cuff disease. *J Shoulder Elbow Surg*. 1996;5(5):383-392.
59. Stone AV, Ma J, Whitlock PW, et al. Effects of botox and neuronox on muscle force generation in mice. *J Orthop Res*. 2007;25(12):1658-1664.
60. Swan M, Sato E, Galatz LM, et al. The effect of age on rat rotator cuff muscle architecture. *J Shoulder Elbow Surg*. 2014;23(12):1786-1791.
61. Thomopoulos S, Williams GR, Soslowsky LJ. Tendon to bone healing: differences in biomechanical, structural, and compositional properties due to a range of activity levels. *J Biomech Eng*. 2003;125(1):106-113.
62. Warner JP, Krushell RJ, Masquelet A, Gerber C. Anatomy and relationships of the suprascapular nerve: anatomical constraints to mobilization of the supraspinatus and infraspinatus muscles in the management of massive rotator-cuff tears. *J Bone Joint Surg Am*. 1992;74(1):36-45.
63. Yamaguchi K, Tetro A, Blam O, et al. Natural history of asymptomatic rotator cuff tears: a longitudinal analysis of asymptomatic tears detected sonographically. *J Shoulder Elbow Surg*. 2001;10(3):199-203.